

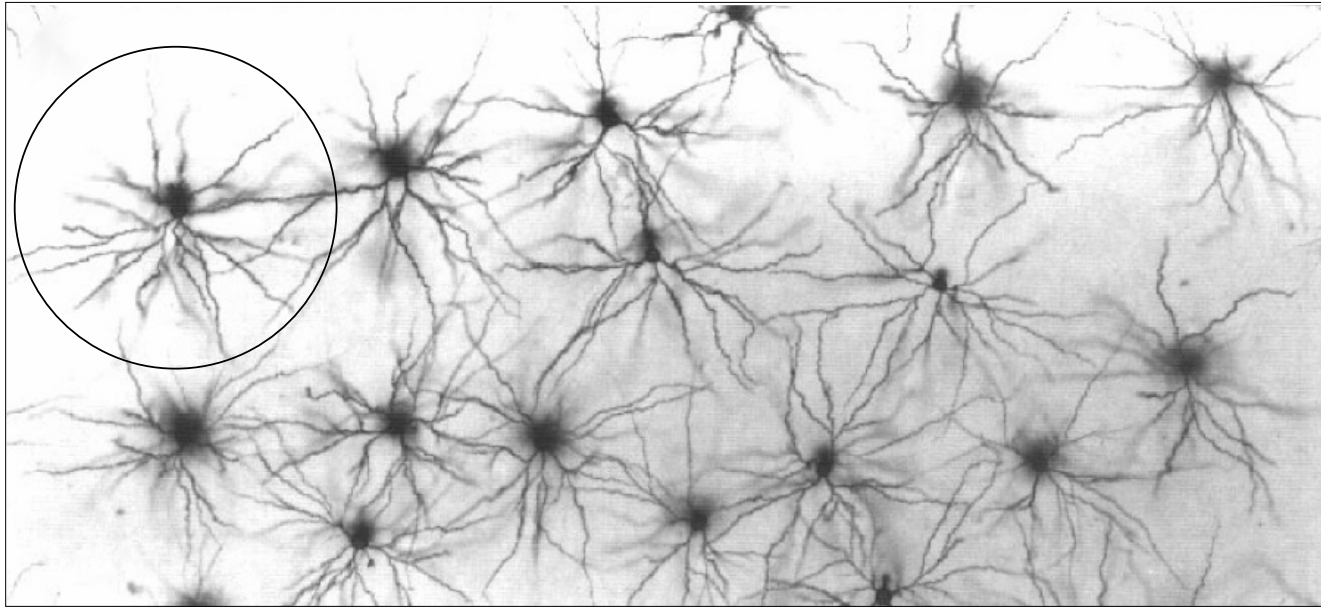
Modeling the Visual System

Dr. James A. Bednar

jbednar@inf.ed.ac.uk

<http://homepages.inf.ed.ac.uk/jbednar>

Sample network to model

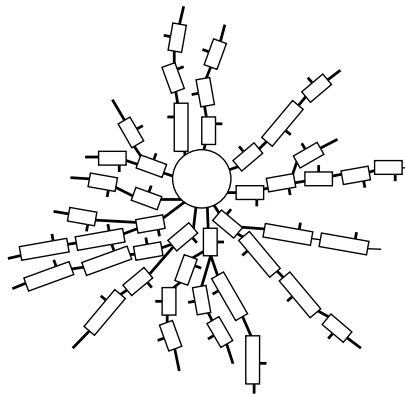


CMVC figure 3.1a

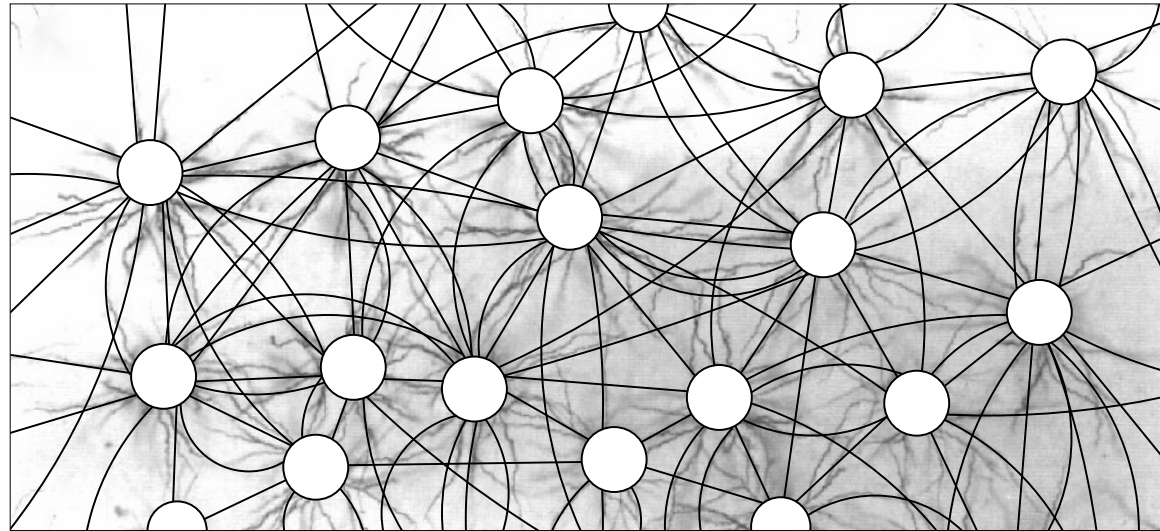
Tangential section with a small subset of neurons labeled

Where do we begin?

Modeling approaches



Compartmental
neuron model



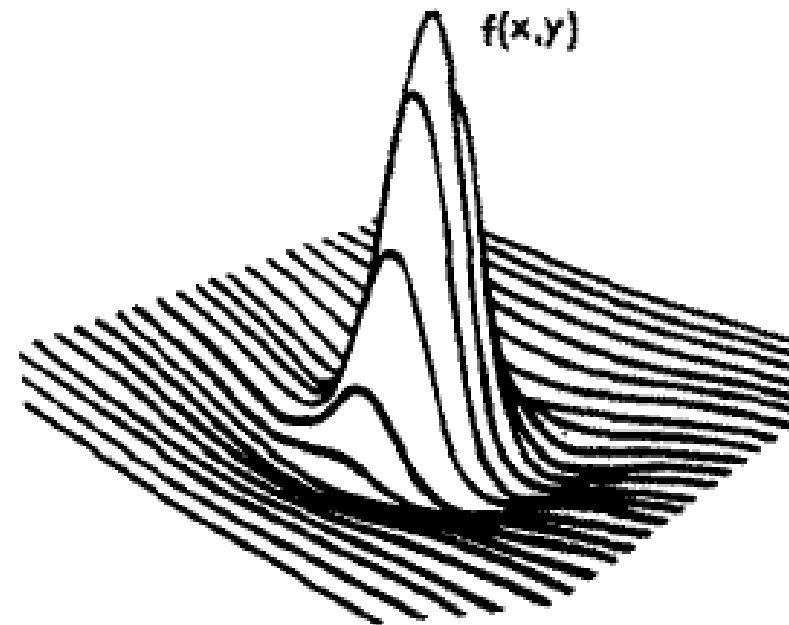
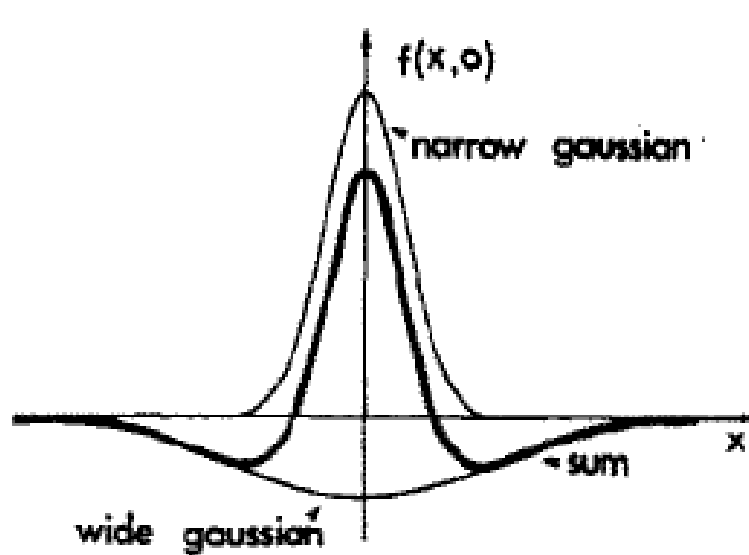
Integrate-and-fire / firing-rate model of the network

CMVC figure 3.1b,e

One approach: model single cells extremely well

Our approach: many, many simple single-cell models

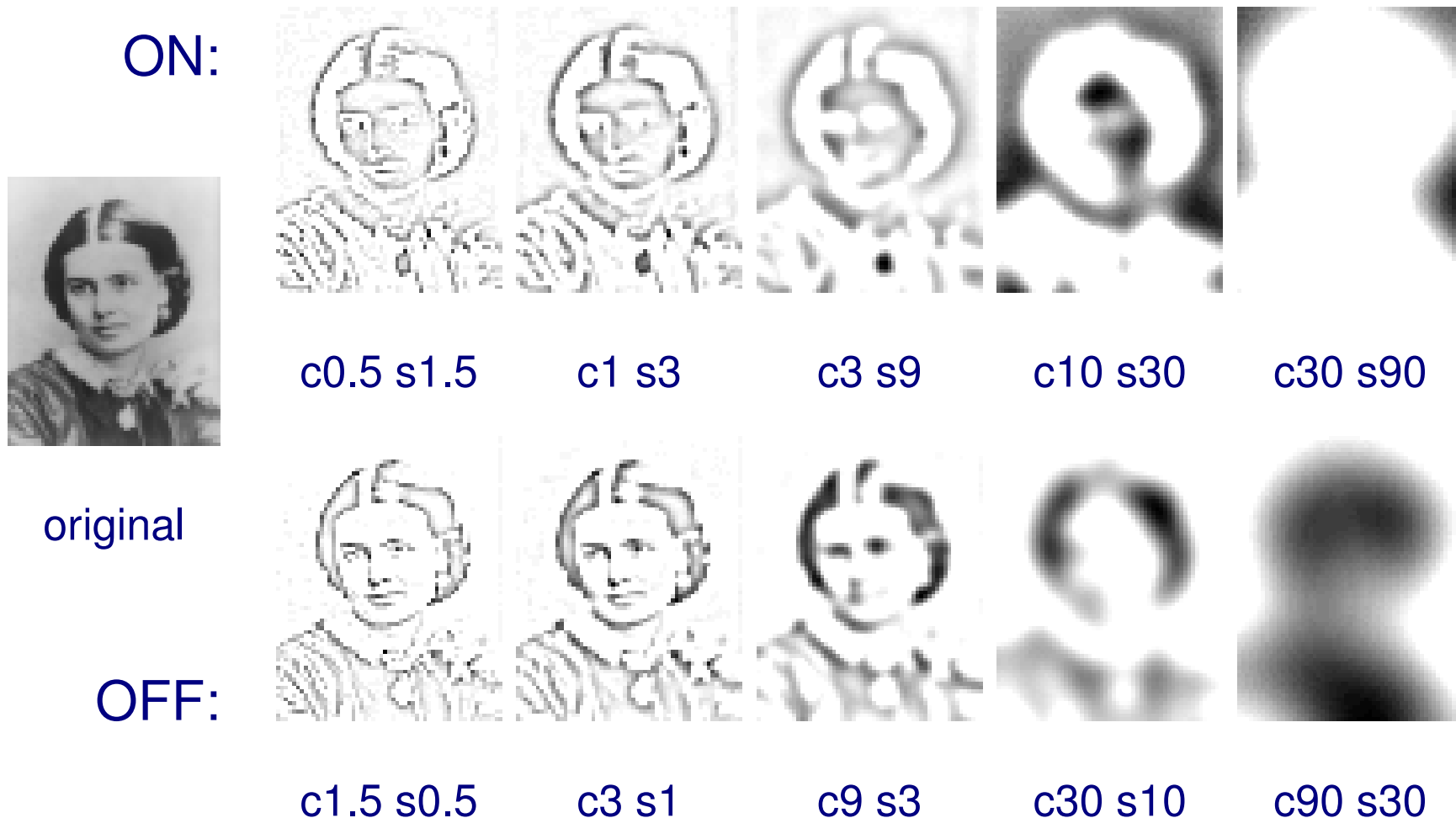
Adult retina and LGN cell models



(Rodieck 1965)

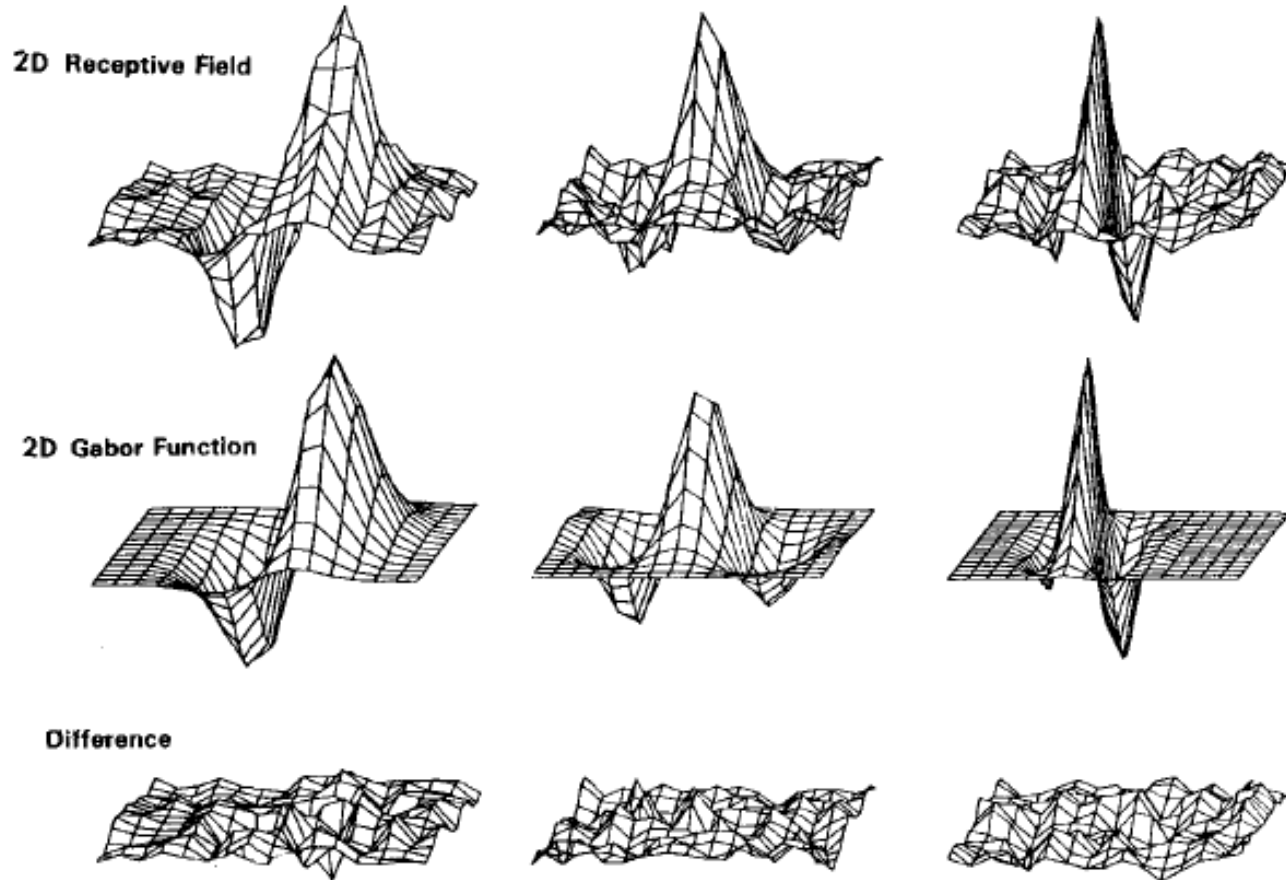
- Standard model of adult RGC or LGN cell activity:
Difference of Gaussians
- Can be tuned for quantitative match to firing rate
- Can add temporal component (transient+sustained)

Effect of DoG



Each DoG, if convolved with the image, performs edge detection at a certain size scale (spatial frequency band)

Adult V1 cell model: Gabor

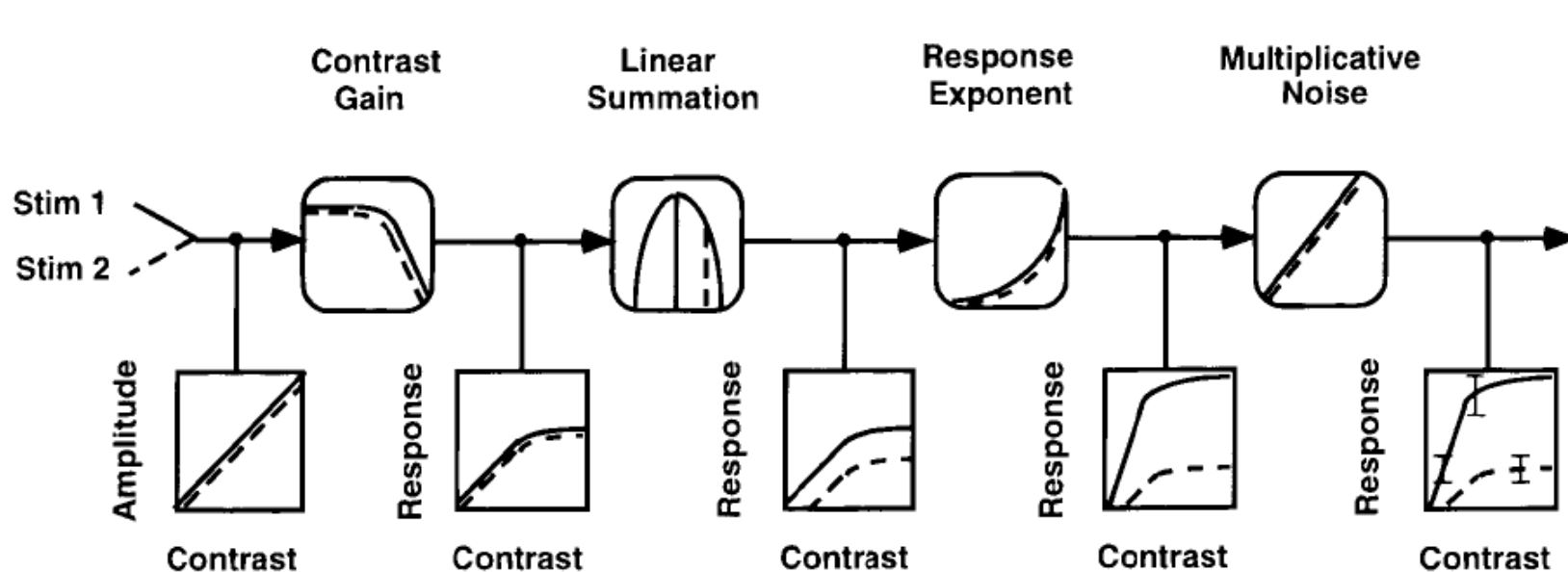


(Adult cat; Daugman 1988)

Standard model of adult V1 simple cell spatial preferences:
Gabor (Gaussian times sine grating) (Daugman 1980)

Adult V1 cell model: CGE

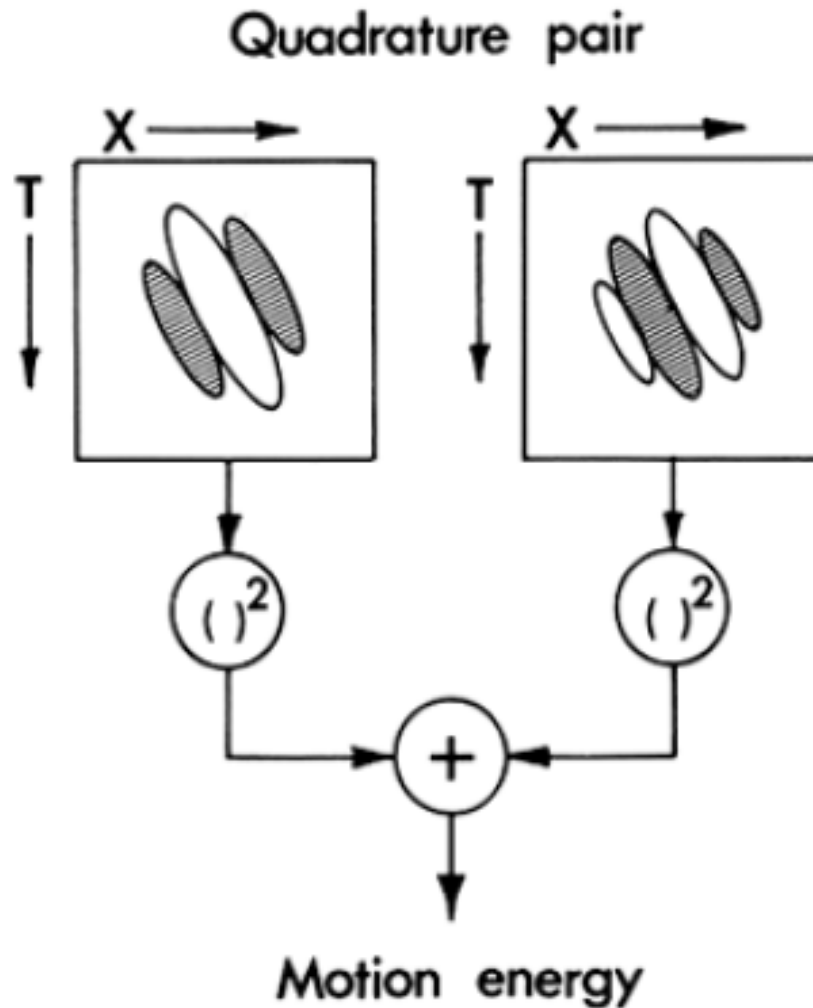
Contrast-Gain Exponent (CGE) Model



(Geisler & Albrecht 1997)

- Gabor model fits spatial preferences
- Simple response function: dot product
- To match observations: need to add numerous nonlinearities
- Example: CGE model (Geisler & Albrecht 1997)

Adult V1 cell model: Energy



- Spatiotemporal energy:
Standard model of
complex cell
(Adelson & Bergen 1985)
- Combines inputs from a
quadrature pair
(two simple cell models
out of phase)
- Achieves phase
invariance

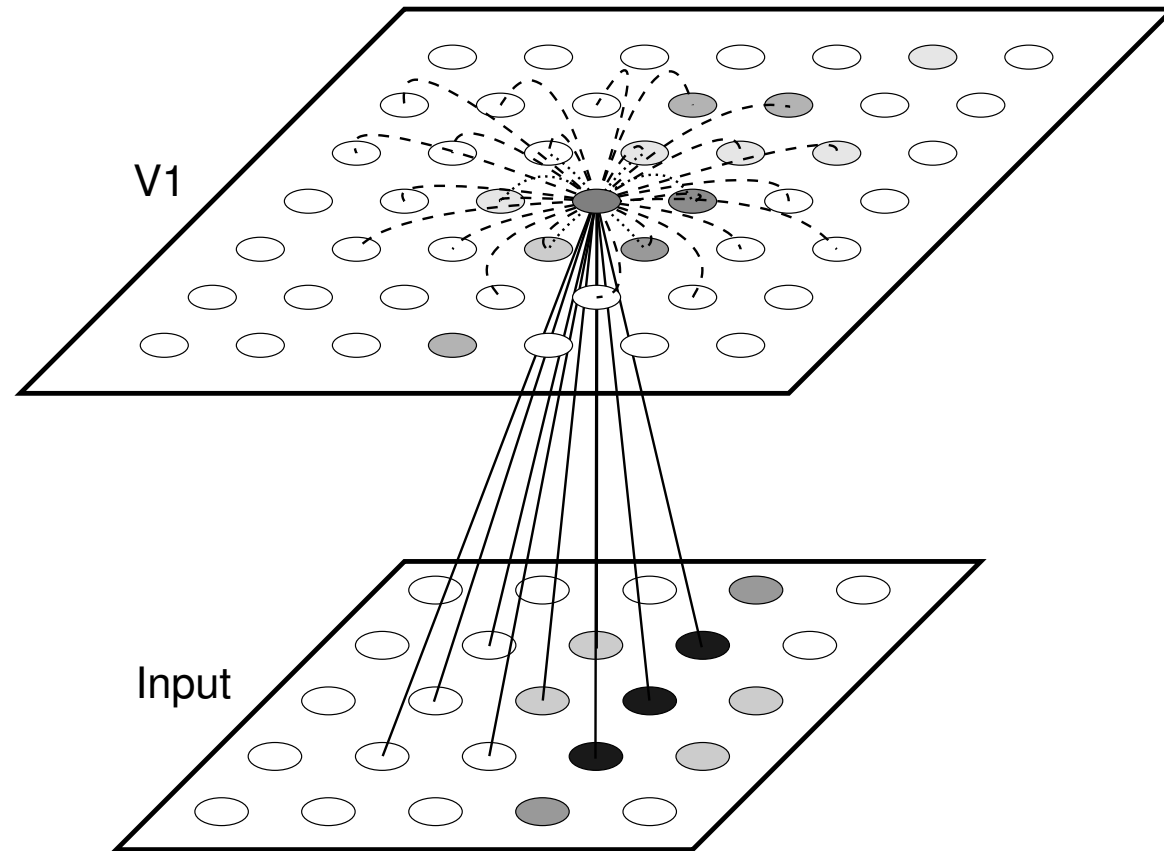
Retina/LGN development models

Relatively rare, but more in recent years:

- Retinal wave generation
(e.g. Feller et al. 1997)
- RGC development based on retinal waves
(e.g. Eglen & Willshaw 2002)
- Retinogeniculate pathway based on retinal waves
(e.g. Eglen 1999; Haith 1998)

Because of the wealth of data from the retina, such models can now become quite detailed.

Our focus: Cortical map models



CMVC figure 3.3

Basic architecture: input surface mapped to cortical surface + some form of lateral interaction

Kohonen SOM: Feedforward

Popular computationally tractable map model (Kohonen 1982)

Feedforward activity of unit (i, j) :

$$\eta_{ij} = \|\vec{V} - \vec{W}_{ij}\| \quad (1)$$

(distance between input vector \vec{V} and weight vector \vec{W})

Not particularly biologically plausible, but easy to compute, widely implemented, and has some nice properties.

Note: Activation function is not typically a dot product; the CMVC book is confusing about that.

Kohonen SOM: Lateral

Abstract model of lateral interactions:

- Pick winner (r, s)
- Assign it activity η_{\max}
- Assume that activity of unit (i, j) can be described by a neighborhood function, such as a Gaussian:

$$h_{rs,ij} = \eta_{\max} \exp \left(-\frac{(r-i)^2 + (s-j)^2}{\sigma_h^2} \right), \quad (2)$$

Models lateral interactions that depend only on distance from winning unit.

Kohonen SOM: Learning

Inspired by basic Hebbian rule (Hebb 1949):

$$w' = w + \alpha \eta \chi \quad (3)$$

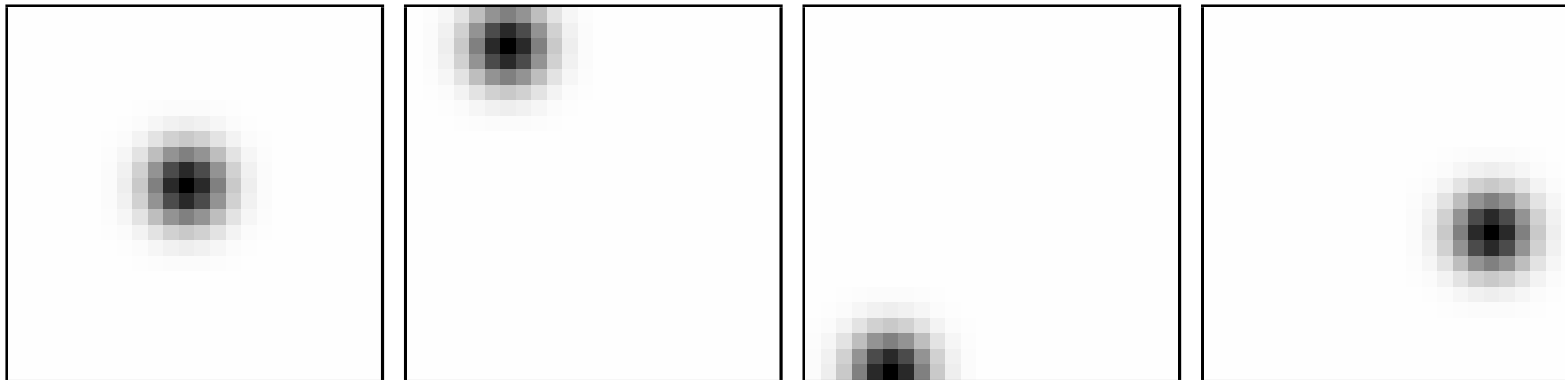
where the weight increases in proportion to the product of the input and output activities.

In SOM, the weight vector is shifted toward the input vector based on the Euclidean difference:

$$w'_{k,ij} = w_{k,ij} + \alpha(\chi_k - w_{k,ij})h_{rs,ij}. \quad (4)$$

Hebb-like, but depending on distance from winning unit

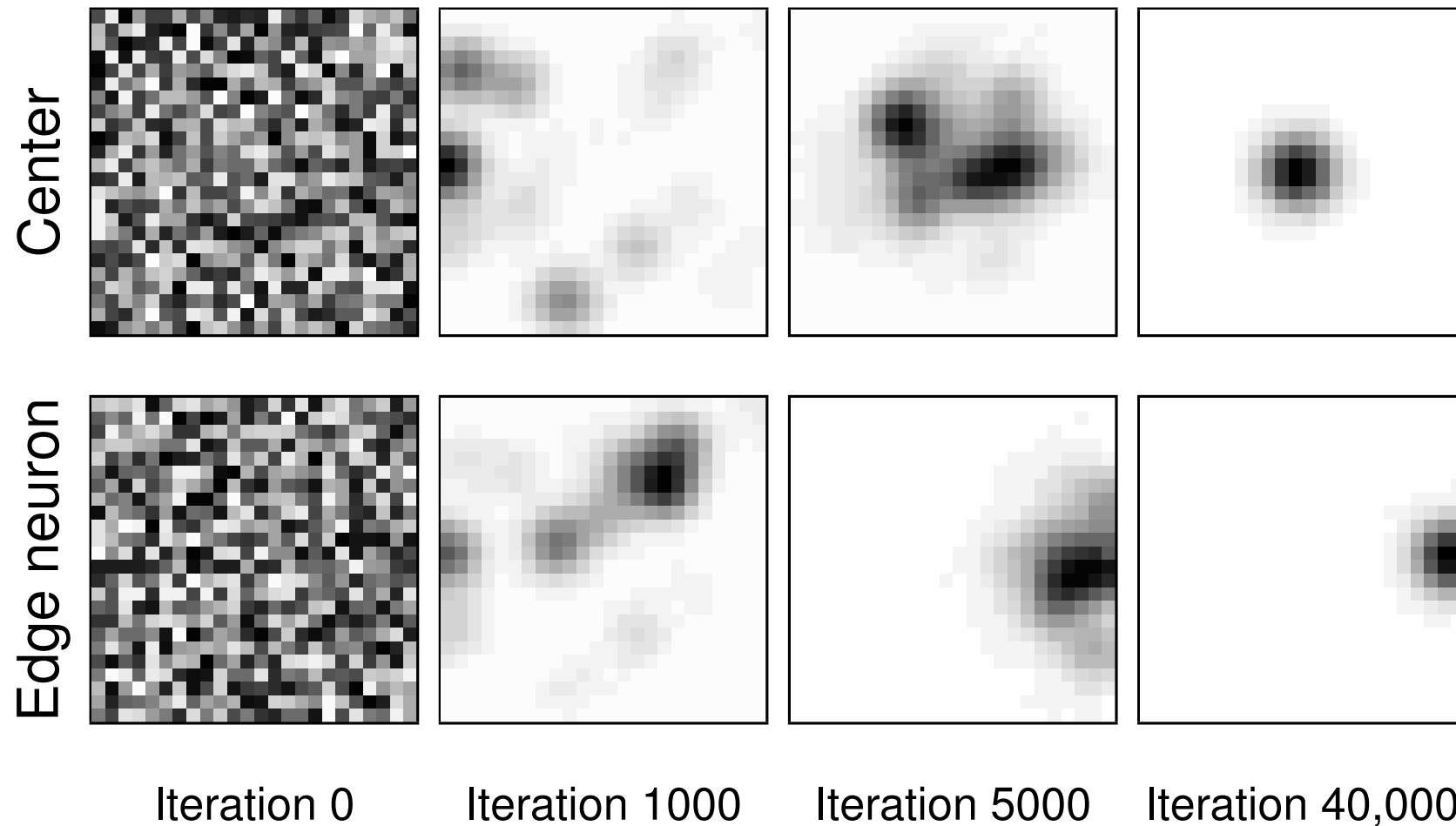
SOM example: Input



CMVC figure 3.4

- SOM will be trained with unoriented Gaussian activity patterns
- Random (x, y) positions anywhere on retina
- 576-dimensional input, but the x and y locations are the only source of variance

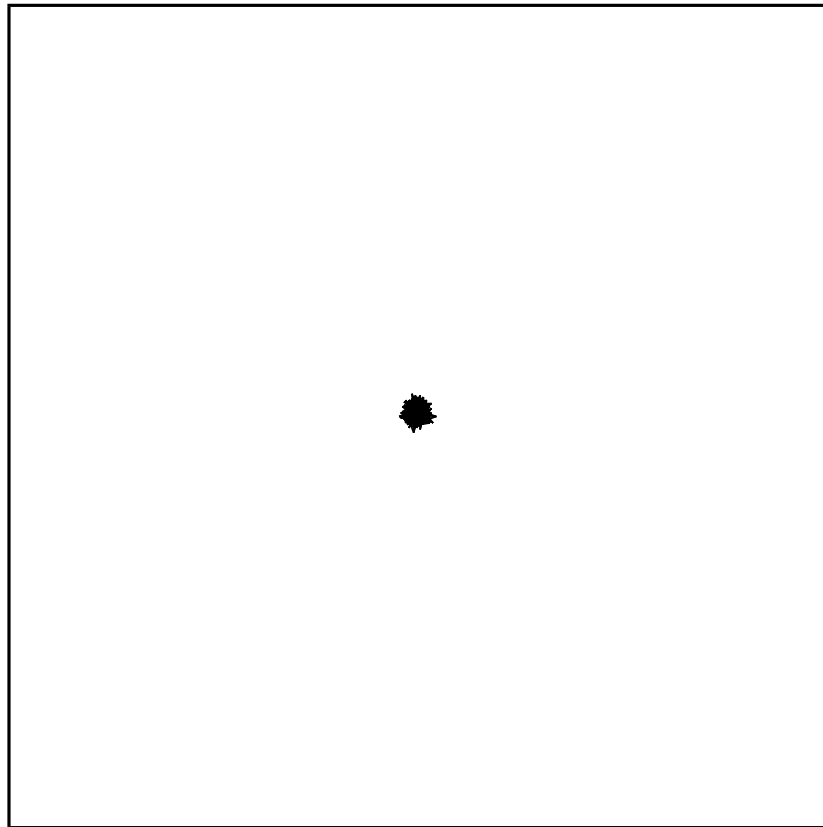
SOM: Weight vector self-org



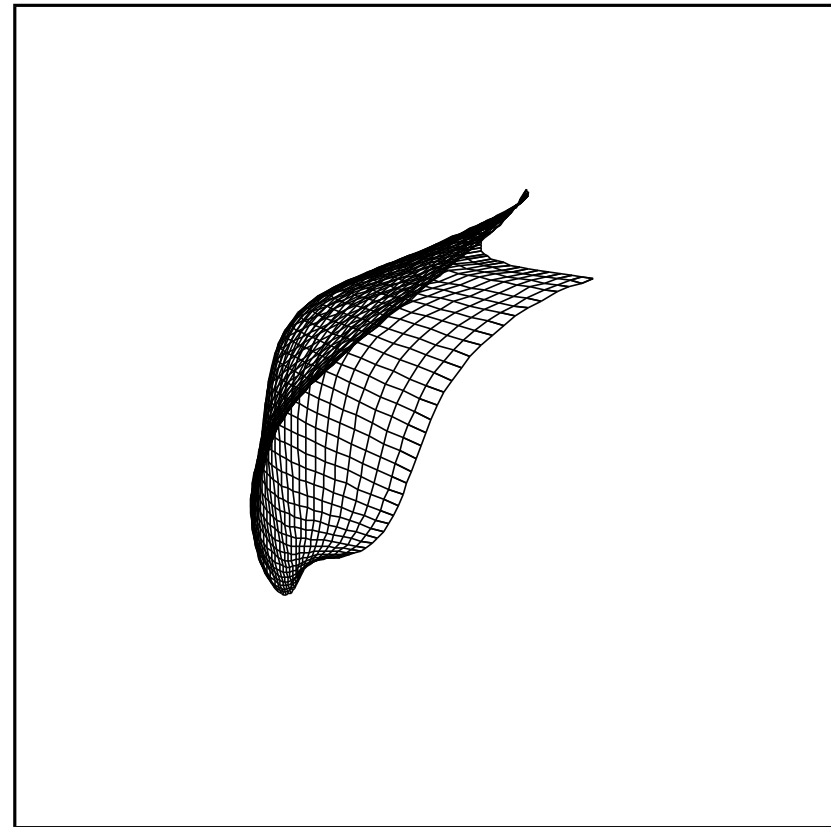
CMVC figure 3.5

Combination of input patterns; eventually settles to an exemplar

SOM: Retinotopy self-org



Iteration 0: Initial



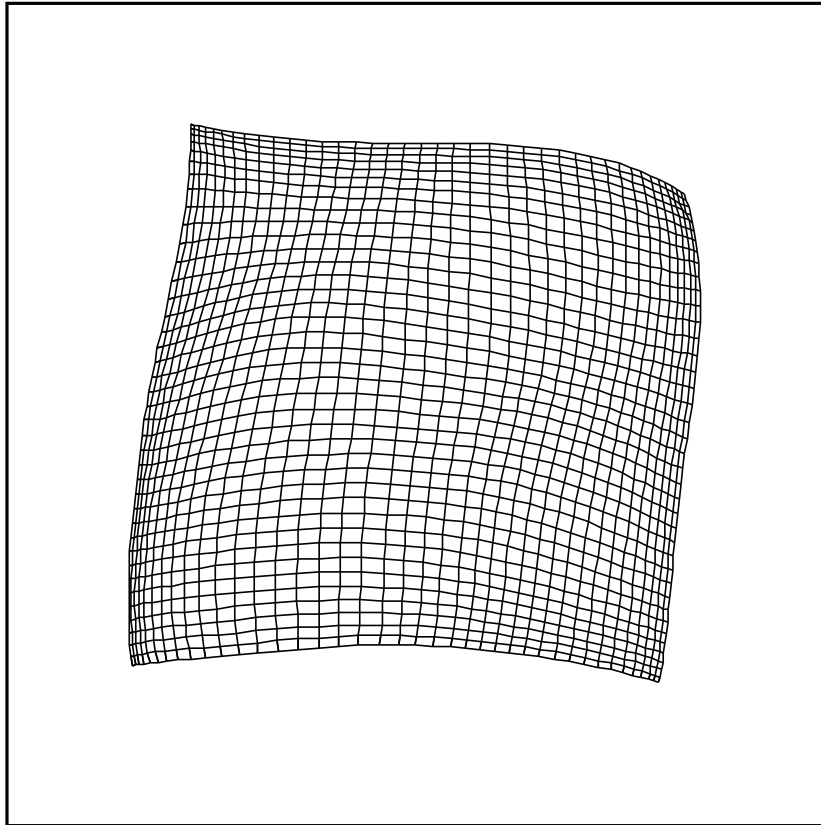
Iteration 1000: Unfolding

Initially bunched (all average to zero)

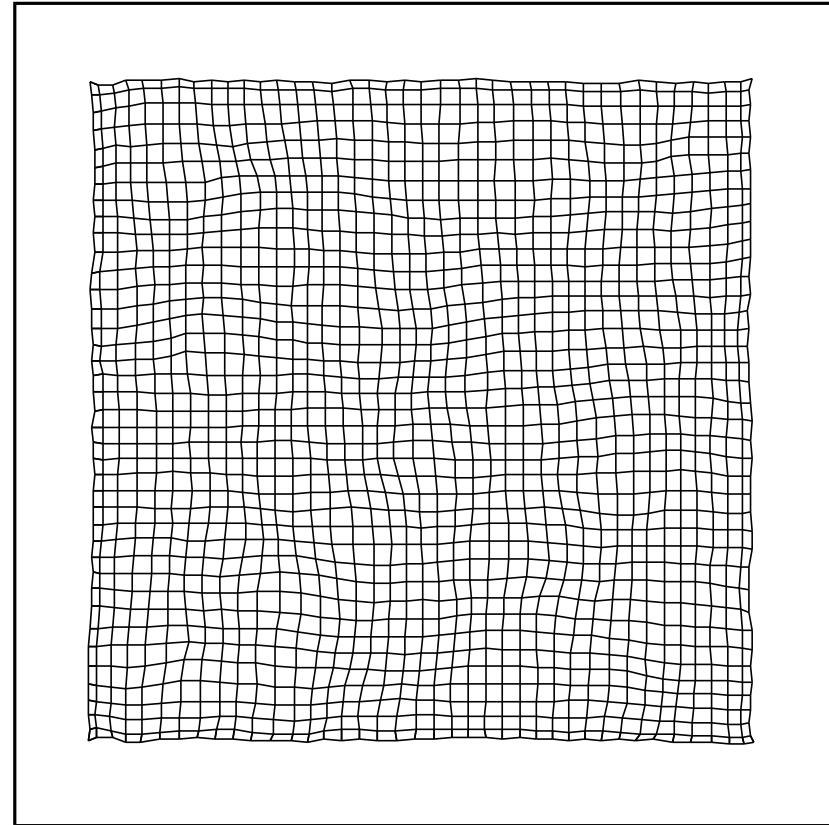
Unfolds as neurons differentiate

CMVC figure 3.6a-b

SOM: Retinotopy self-org



Iteration 5000: Expanding

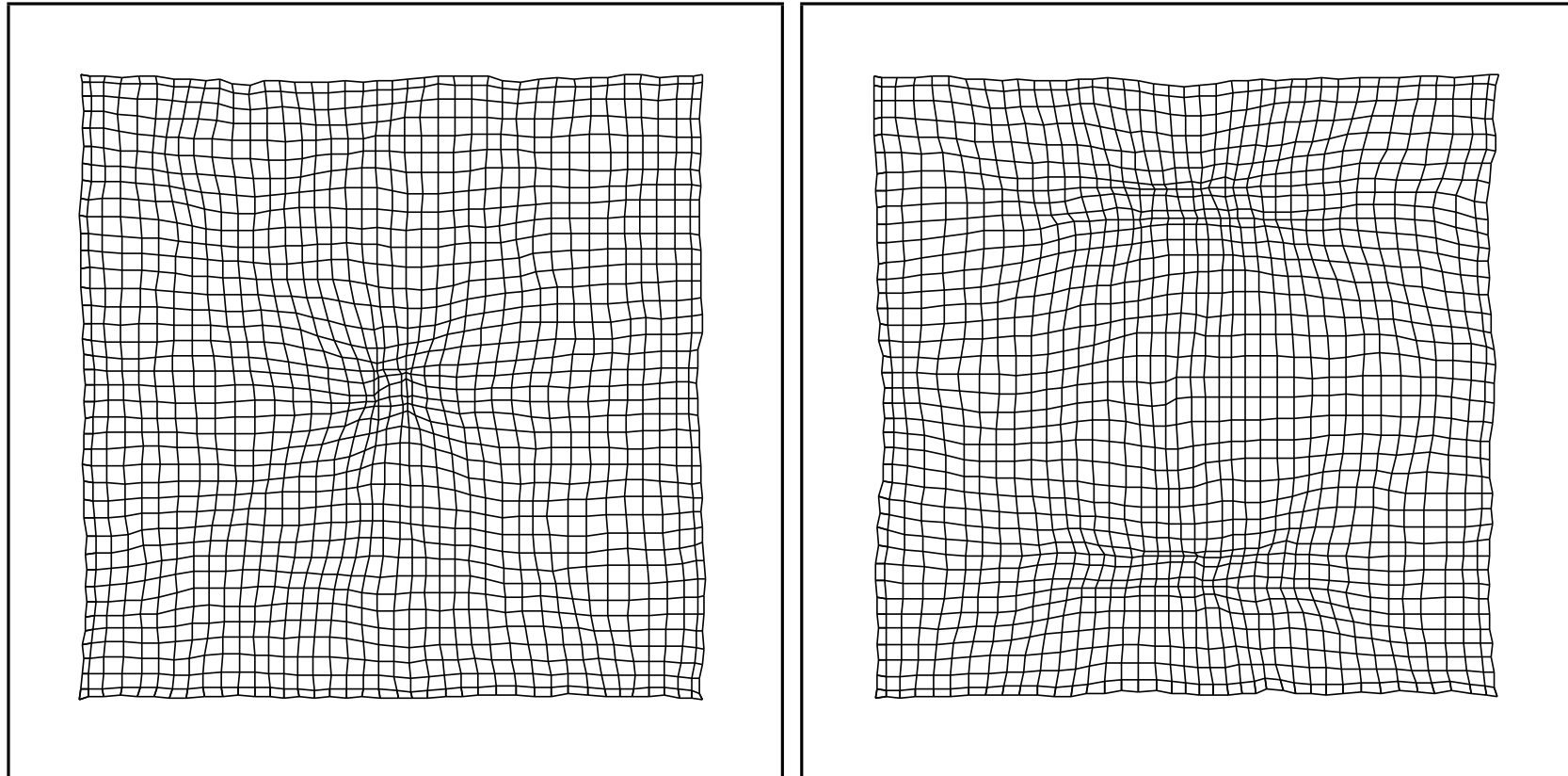


Iteration 40,000: Final

Expands to cover usable portion of input space.

CMVC figure 3.6c-d

Magnification of dense input areas



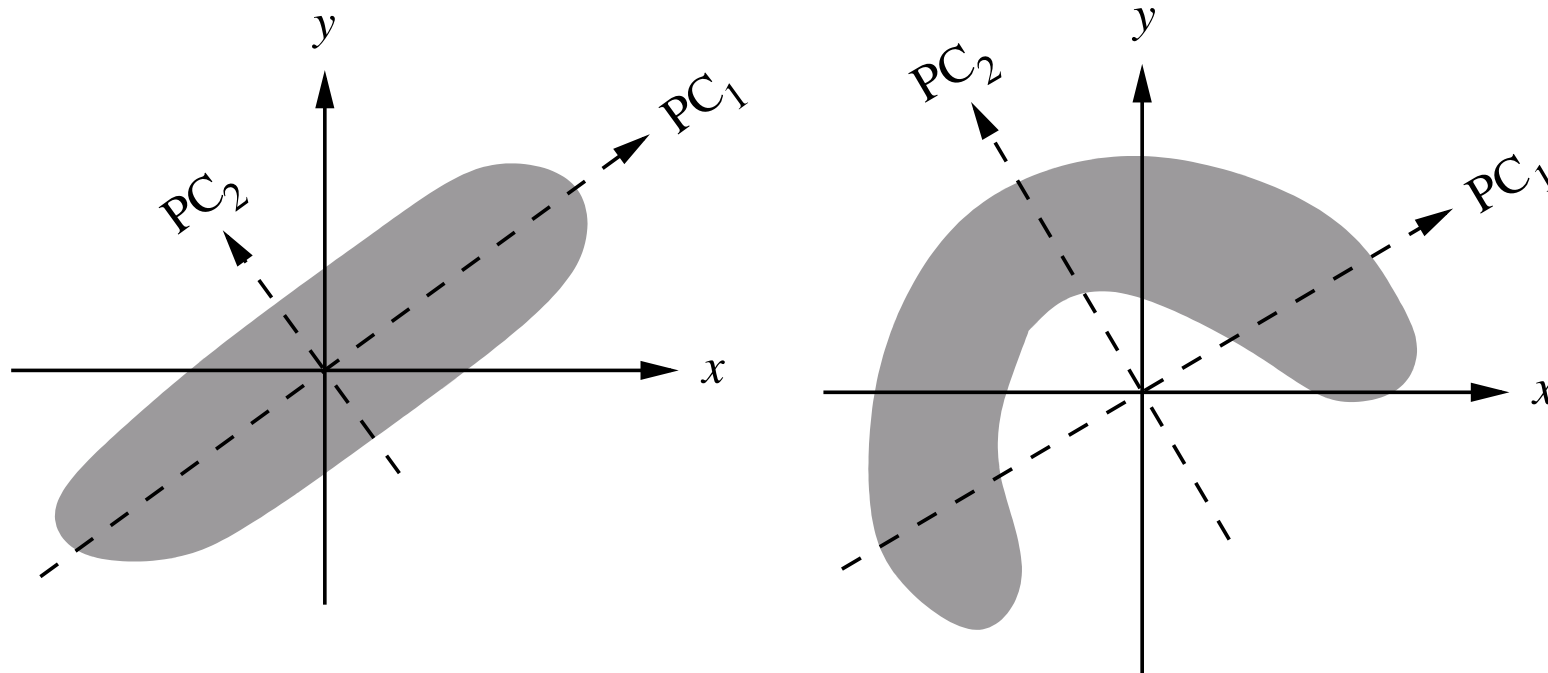
CMVC figure 3.7

Gaussian distribution

Two long Gaussians

Density of units receiving input from a particular region
depends on input pattern statistics

Principal components of data distributions



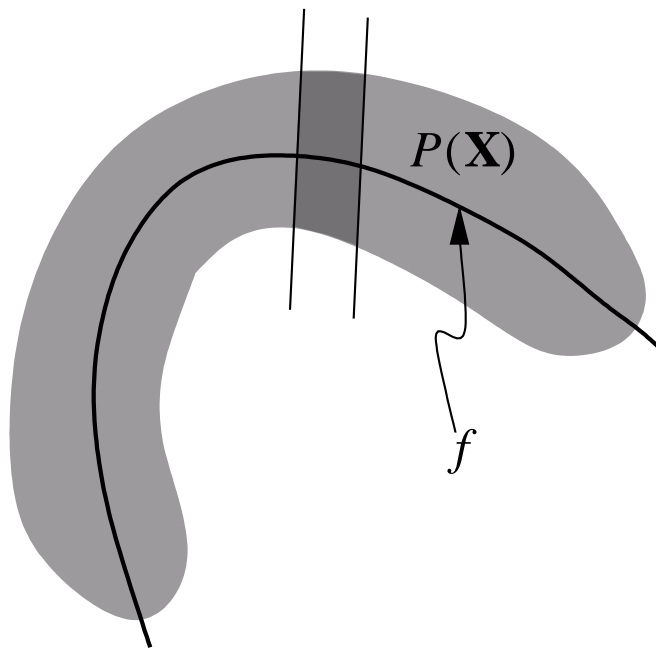
(a) Linear distribution

(b) Nonlinear distribution

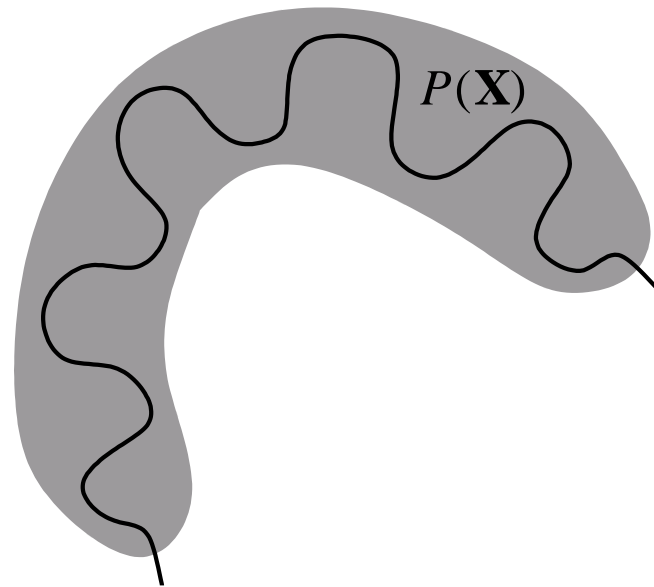
CMVC figure 3.8

PCA: linear approximation, good for linear data

Nonlinear distributions: principal curves, folding



Principal curve



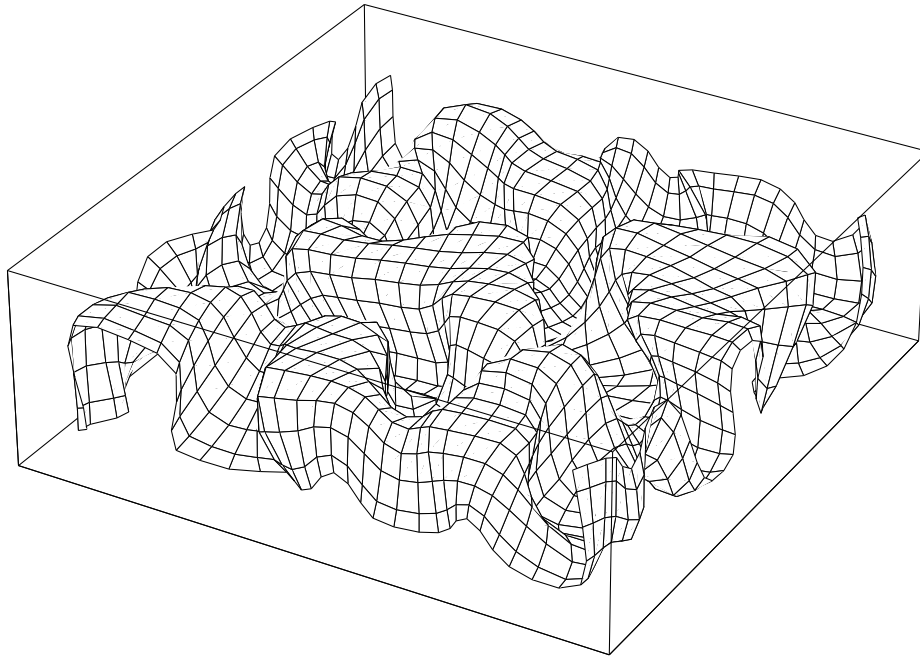
Folded curve

Generalization of idea of PCA to pick best-fit curve(s)

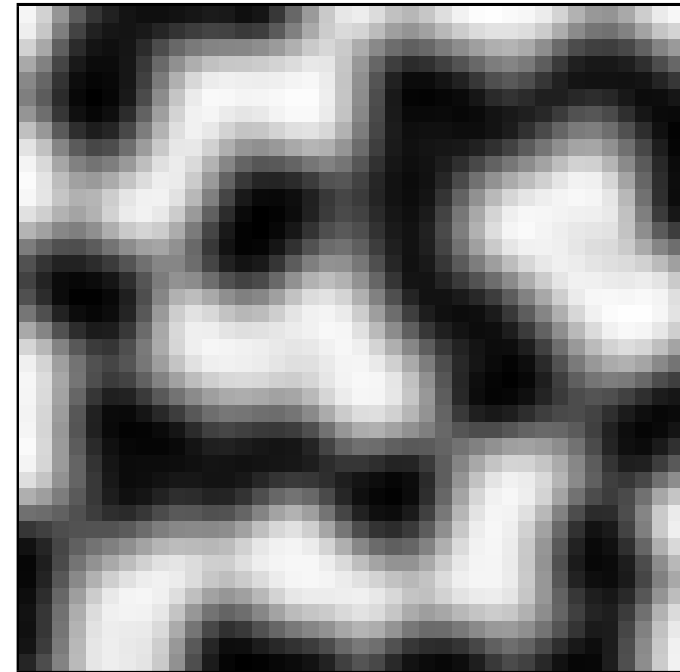
Multiple possible curves

CMVC figure 3.9

Three-dimensional model of ocular dominance



Representing the third dimension by
folding

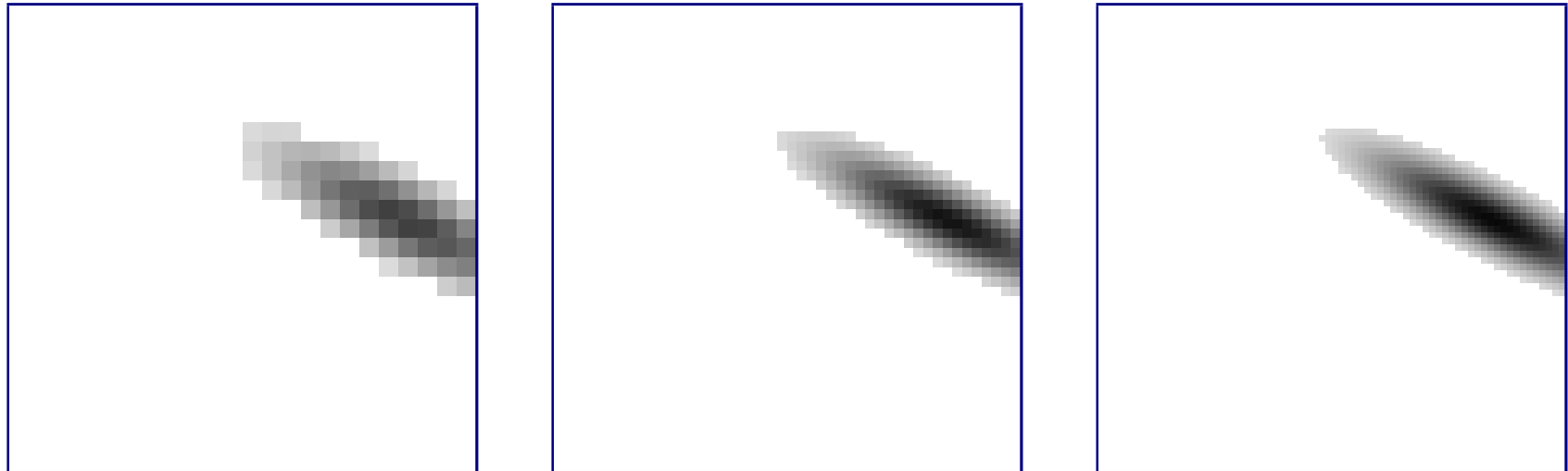


Visualization of ocular
dominance

CMVC figure 3.10

Feature maps: Principal surfaces?

Role of density of input sheet



- Gaussian inputs are nearly band-limited
(since Fourier transform is also Gaussian)
- Density of input sampling unimportant, if it's greater than 2X highest frequency in input (Nyquist theorem)

Role of density of SOM sheet

SOM sheet acts as a discrete approximation to a two-dimensional surface.

How many units are needed for the SOM depends on how nonlinear the input distribution is — a smoothly varying input distribution requires fewer units to represent the shape.

Only loosely related to the input density — input density limits how quickly the input varies across space, but only for wideband stimuli.

Summary

- Basic intro to visual modeling
- Adult models are well established, but vision-specific
- SOM: maps multiple dimensions down to two
- Feature maps: Principal surfaces?

References

- Adelson, E. H., & Bergen, J. R. (1985). Spatiotemporal energy models for the perception of motion. *Journal of the Optical Society of America A*, 2, 284–299.
- Daugman, J. G. (1980). Two-dimensional spectral analysis of cortical receptive field profiles. *Vision Research*, 20, 847–856.
- Daugman, J. G. (1988). Complete discrete 2-D Gabor transforms by neural networks for image analysis and compression. *IEEE Transactions on Acoustics, Speech, and Signal Processing*, 36 (7).
- Eglen, S. J. (1999). The role of retinal waves and synaptic normalization

in retinogeniculate development. *Philosophical Transactions of the Royal Society of London Series B*, 354 (1382), 497–506.

Eglen, S. J., & Willshaw, D. J. (2002). Influence of cell fate mechanisms upon retinal mosaic formation: A modelling study. *Development*, 129 (23), 5399–5408.

Feller, M. B., Butts, D. A., Aaron, H. L., Rokhsar, D. S., & Shatz, C. J. (1997). Dynamic processes shape spatiotemporal properties of retinal waves. *Neuron*, 19, 293–306.

Geisler, W. S., & Albrecht, D. G. (1997). Visual cortex neurons in monkeys and cats: Detection, discrimination, and identification. *Visual Neuroscience*, 14 (5), 897–919.

Haith, G. L. (1998). *Modeling Activity-Dependent Development in the Retinogeniculate Projection*. Doctoral Dissertation, Department of Psychology, Stanford University, Palo Alto, CA.

Hebb, D. O. (1949). *The Organization of Behavior: A Neuropsychological Theory*. Hoboken, NJ: Wiley.

Kohonen, T. (1982). Self-organized formation of topologically correct feature maps. *Biological Cybernetics*, 43, 59–69.

Rodieck, R. W. (1965). Quantitative analysis of cat retinal ganglion cell response to visual stimuli. *Vision Research*, 5 (11), 583–601.